

LABORATORY OF NUCLEAR MEDICINE AND RADIATION BIOLOGY
900 VETERAN AVENUE
UNIVERSITY OF CALIFORNIA, LOS ANGELES, CALIFORNIA 90024
AND DEPARTMENT OF RADIOLOGICAL SCIENCES
UCLA SCHOOL OF MEDICINE, LOS ANGELES, CALIFORNIA 90024

This manuscript is a contribution to the monograph edited by Daniel S. Berman and Dean Mason, entitled "Clinical Nuclear Cardiology".

These studies were supported by Contract #DE-AM03-76-SF00012 between the U.S. Department of Energy and the University of California

Prepared for the U.S. Department of Energy
under Contract #DE-AM03-76-SF00012

POSITRON EMISSION TOMOGRAPHY
OF THE HEART

Heinrich R. Schelbert, M.D., Michael E.
Phelps, Ph.D. and David E. Kuhl, M.D.

DISCLAIMER

This report was prepared as an account of work sponsored by an agency of the United States Government. Neither the United States Government nor any agency thereof, nor any of their employees, make any warranty, express or implied, or assumes any legal liability or responsibility for the accuracy, completeness, or usefulness of any information, apparatus, product, or process disclosed, or represents that its use would not infringe privately owned rights. Reference herein to any specific commercial product, process, or service by trade name, trademark, manufacturer, or otherwise does not necessarily constitute or imply its endorsement, recommendation, or favoring by the United States Government or any agency thereof. The views and opinions of authors expressed herein do not necessarily state or reflect those of the United States Government or any agency thereof.

DISCLAIMER

Portions of this document may be illegible in electronic image products. Images are produced from the best available original document.

Positron emission computed tomography (PCT) represents an important new tool for the noninvasive evaluation and, more importantly, quantification of myocardial performance. Most currently available techniques permit assessment of only one aspect of cardiac function, i.e. myocardial perfusion by gamma scintillation camera imaging with Thallium-201 or left ventricular function by echocardiography or radionuclide angiocardiology. With PCT it may become possible to study all three major segments of myocardial performance, i.e. regional blood flow, mechanical function and, most importantly, myocardial metabolism. Each of these segments can either be evaluated separately or in combination. It is conceivable that with this new study means the metabolic link between flow and mechanical function can be established. PCT, thus, may provide not only heretofore unavailable information on local myocardial metabolism but greatly improve our understanding of the interdependency of flow, metabolism and mechanical function in the normal and diseased heart.

The unique capability of PCT is the result of two developments: a) the technical innovations of the imaging device; and b) the availability of specific radioactive tracers for flow and/or metabolism. Because PCT has entered the field of cardiology only recently and is still largely unknown, we shall briefly describe the principles and technological advantages of the imaging device, review currently available radioactive tracers and how they can be employed for the assessment of flow, function and metabolism; and, lastly, discuss possible applications of PCT for the study of cardiac physiology or its potential role in the diagnosis of cardiac disease.

A. TECHNICAL CONSIDERATIONS

The Positron Emission Computed Tomograph

PCT visualizes the distribution of radioactive tracers in the body or within organs in form of quantitative cross-sectional images that reflect the tracer tissue concentrations in terms of mCi or mg per gram tissue. These images are therefore comparable to autoradiographs that can be obtained in vivo or provide a capability that is similar to in-vitro counting of tissue samples. This capability is due to the depth-independent resolution and an appropriate correction for photon attenuation which together with the three-dimensional display represent the main technological advantages of PCT over conventional gamma camera imaging (1-3). They are based upon the principles of annihilation coincidence detection.

Positrons are particles with the mass of an electron but an opposite charge. As the positron loses kinetic energy, it interacts with an electron, and both particles are annihilated. Their mass is converted into two 511 KeV photons that leave the site of interaction in diametrically opposed directions (Figure 1). The annihilation is recorded by two opposed scintillation detectors connected by a coincidence circuit. Only interactions occurring within well the defined field of coincidence detection between the two detectors are recorded. This unique "electronic collimation" accounts for the depth independent resolution of PCT. Prior to reaching the detectors the 511 KeV photons are attenuated. As shown in Figure 1, attenuation is a function of the total path length ($a+b$) and an attenuation coefficient (μ) that is specific for various tissues. By placing a positron emitting source between the detector and the patient, the total attenuation of 511 KeV photons can be measured and used for correction of photon attenuation as the tomographic images are reconstructed.

The simultaneous emission of two annihilation photons in diametrically opposed directions and their recording by detectors pairs in coincidence form

the basis of PCT. During imaging, data are collected by performing linear scans at discrete angles throughout a 180° arc around the patient. A number of prototype positron imaging devices has been designed in the past (Figure 2). State of the art PCT's are exemplified by systems with hexagonal, octagonal or circular arrays of scintillation detector pairs. For image reconstruction, these devices employ algorithms that are similar to those used in conventional transmission computed tomography (CT).

The device used in our laboratory at UCLA is the first commercially available whole body positron emission computed axial tomograph (Figure 3) and has been described in detail previously ⁽⁴⁾. Its imaging gantry consists of six banks of each 11 NaI(Tl) detectors arranged in hexagonal form. Cross-sectional imaging is performed in the high (0.95 cm FWHM), medium (1.3 cm) or low resolution mode (1.7 cm). The resolution in the axial direction or "slice thickness" is approximately 1.8 cm. In addition to tomographic images, rectilinear scans can be obtained for easier selection of the appropriate cross-sectional levels.

An imaging procedure is typically begun with a rectilinear transmission scan in order to assign the starting level for tomographic imaging. The operator then selects number and spacing of the desired cross-sections, scan time and resolution mode and records a set of contiguous cross-sectional transmission images. The radioactive tracer is then administered and the data for a set of cross-sectional emission images at exactly the same levels acquired. Although the system is capable of acquiring scans at a rate of 10 seconds, images are typically recorded over a 2 to 10 minute period in order to obtain statistically sufficient counts. A sequence of six cross-sections at 1.5 cm intervals, for instance of the heart, is usually completed within 20 minutes, with each image containing 600,000 to 2,000,000 counts (for a dose of

15 to 30 mCi) (Figure 4).

During image reconstruction corrections are made for photon attenuation using the initial transmission images. The cross-sectional images are displayed on the TV-monitor. Regional tissue concentrations of radioactive tracers can be determined by the operator from regions-of-interest. The device also provides the capability of data acquisition in the gated mode. The PCT is synchronized with the patients' ECG and the cardiac cycle divided into 16 segments. Data from each consecutive phase are collected into separate buffer memories and - following reconstruction - displayed in cine mode as a sequence of image frames that clearly demonstrates regional wall motion and wall thickening. Gated imaging further removes motion artifacts and considerably improves visualization of anatomical details (Figure 5).

Radiopharmaceuticals

As the development of new tomographic imaging devices proceeded a whole family of new radiopharmaceuticals emerged that are highly specific for blood flow or various metabolic pathways and, hence, offer for the first time a capability for the in-vivo quantification of local organ metabolism. As we will see, the uniqueness of these radioactive tracers is that they represent naturally occurring metabolic substrates or their analogs labeled with positron emitting isotopes such as oxygen-15, nitrogen-13, carbon-11 or fluorine-18 (Table I). The radioactive label does not alter the biological behavior of these compounds and therefore permit evaluation and measurement of metabolic pathways. Table 1 lists positron emitting isotopes currently in use. To date the relatively short physical halftime represents one of the major limitations for a more wide spread use of PCT. These halftimes range from 2 to 110 minutes and necessitate on-site production and, thus, an on-site cyclotron. On the other hand there are advantages to the short half-time: the radiation

does to the patient is small and studies can be repeated at short time intervals.

The dependency for on-site accelerators can be bypassed to some degree by generator systems (6-9). With their use a number of isotopes suitable for PCT can be obtained in a manner much like the widely used technetium-99m that is simply eluted from the Mo-99 \rightarrow Tc-99m generator. Thus far however, these generators provide only a limited number of positron emitting isotopes (Table 1). Furthermore, incorporation of these isotopes into organic or physiologic compounds has not been accomplished yet without modifying their physiologic behavior.

Despite the fact that PCT has become available only a few years ago an impressive number of radiopharmaceuticals has already been developed. As listed in Table II, these radiopharmaceuticals can be broadly defined as blood pool labeling agents, blood flow indicators and metabolic tracers. While in fact almost any metabolic substrate could be labeled with either O-15, N-13 or C-11 and the number of potentially useful indicators appears unlimited, Table II lists only those that have been at least to some degree evaluated in the in-vivo situation or have been employed in conjunction with PCT. The potential usefulness of some of these compounds is self-evident although many await further and more rigorous evaluation before they can be employed with PCT. Further, while labeled amino acids appear potentially useful for evaluating protein metabolism (10), in the subsequent discussion we will focus only on C-11 palmitate and F-18 deoxyglucose both of which - because glucose and free fatty acids are the main energy substrates for myocardium - seem of particular interest to the study of the heart. In addition, we will review agents that can be used for evaluating ventricular function and regional myocardial blood flow.

B. POSITRON EMISSION TOMOGRAPHY FOR THE STUDY OF CARDIAC PERFORMANCE

a) Regional myocardial blood flow

We emphasized earlier the autoradiographic nature of the cross-sectional images which reflect the distribution of tracer tissue concentrations in a quantitative manner and, hence, can be used to measure indicator tissue concentrations in-vivo in terms of mCi per gram tissue. This capability is comparable to tissue sampling and in vitro counting techniques and therefore lends itself the measurement of regional myocardial perfusion with radioactive labeled microspheres by means of the arterial reference technique.

The quantitative capability of PCT is however somewhat limited by the partial volume effect which Hoffman et al ⁽¹¹⁾ recently demonstrated in phantom studies. For example if two objects with the same indicator concentrations but of different sizes were imaged quantitatively PCT would underestimate the concentration of the smaller object. This is particularly important for studies of the heart because the left ventricular wall is only 0.8 to 2.0 cm thick or about two times less than the spatial resolution of the imaging device. PCT therefore underestimates myocardial tissue concentrations by approximately 50%. Nevertheless, if one establishes a quantitative relationship between concentration recovery by PCT and the object size the loss of concentration recovery can be adequately corrected for once the object size is known. Wisenberg et al ⁽¹²⁾ in our laboratory have demonstrated that this is indeed possible for the heart. In animal experiments regional myocardial tracer tissue concentrations were measured in vivo with a high degree of accuracy after the image concentrations were corrected for wall thickness determined post-mortem or by echocardiography. By correcting the tissue concentrations in this manner the same investigators further confirmed the capability of PCT for the in vivo quantification of regional myocardial blood

flow. They injected Ga-68 labeled albumin microspheres ⁽¹³⁾ into the left atrium and employing the arterial reference technique ⁽¹⁴⁾ they were able to measure accurately regional myocardial blood flow in vivo from ECG gated cross-sectional images of the left ventricular myocardium. These measurements were performed over a flow range from near zero to 500ml/min/100gm. The slope of the regression line between the in vivo and in vitro measurements was near unity (0.99) and the standard error of the estimate only 12ml/min/100gm.

While particulate indicators such as radioactive microspheres are most accurate for measurement of myocardial perfusion their use in man is limited for obvious reasons. In order to apply these studies in man a diffusible indicator is needed that can be administered intravenously, readily crosses the pulmonary vascular bed and then becomes trapped in myocardium in proportion to blood flow. A number of agents recently have become available that may meet these requirements. Among these are potassium-38⁽¹⁵⁾ which is likely to exhibit the same characteristics as potassium-43 used in the past as a flow indicator with gamma camera imaging. Budinger et al ⁽¹⁶⁾ have recently proposed the use of the short-lived Rb-82 which can be obtained from a Sr-82 generator system. This agent again is likely to possess properties that are quite similar to those of Potassium-43 or Rubidium-81 both of which have been used in the past for the assessment of regional myocardial perfusion by standard imaging techniques. Initial results with this agent are promising, yet its ultrashort physical halftime may require specifically designed administration schedules.

Another interesting and recently proposed approach for measuring regional myocardial blood flow by PCT is the exponential infusion of O-15 water or C-11 butanol ⁽¹⁷⁾. Used in the isolated heart preparation these two agents appear promising for the external quantification of myocardial blood flow yet their

utility for use in the in vivo situation with indicator recirculation and blood pool activity awaits further testing and evaluation.

We have extensively evaluated another agent for its suitability as an indicator of regional myocardial blood flow. N-13 ammonia has been proposed initially as a myocardial imaging agent (18-21). Administered intravenously it distributes in proportion to blood flow and rapidly and almost completely clears from blood into myocardium where it is trapped sufficiently long to permit quantitative imaging (Figure 6) (22). With these properties N-13 ammonia resembles to some degree a particulate indicator. At control flow (80ml/min/100gm) the extraction fraction of N-13 ammonia during a single capillary transit approaches 90% (20,21) but decreases as flow increases. Within the range of physiologically occurring flows, i.e. from 80 to 300ml/min/100gm, myocardial tissue concentrations were almost linearly related to myocardial blood flow (Figure 7). Except for extreme changes in arterial plasma pH trapping of N-13 ammonia by myocardium remained unaffected by alterations in the metabolic or functional state of the heart (unpublished data). There is evidence that because of the rapid trapping and fixation of N-13 ammonia in myocardium and the fast clearance from blood (blood levels are less than 2% of peak activity within 5 minutes of injection) noninvasive quantification of regional myocardial blood flow with this agent indeed may be feasible (22).

b) Assessment of regional myocardial function

Traditionally, regional myocardial function is determined from the extent and time course of regional systolic wall motion and thickening and can be derived from contrast cineventriculograms, by echocardiography or by gated blood pool imaging. Similar to conventional gated blood pool imaging the PCT can be synchronized with the patient's ECG and gated cross-sectional images of

the left-ventricular blood pool or the left ventricular myocardium be obtained either at enddiastole and endsystole or even as a sequence of images depicting the entire cardiac cycle (5).

The cardiac blood pools can readily be visualized by inhalation of small amounts of C-11 carbon monoxide. Attached to hemoglobin as carboxyhemoglobin this agent represents an excellent blood pool imaging agent. Gated images of the left and right ventricular cavities can be obtained with the PCT and regional left and right ventricular function assessed. It would appear that quantification of global as well as regional left ventricular function from these images will be possible by reconstructing a three-dimensional image of the left ventricular cavity.

Moreover, it appears that regional wall thickening is a highly sensitive index of regional function that can be determined from gated cross-sectional images of the left ventricular myocardium (Figure 5). We mentioned earlier the difficulties with the object size related concentration recovery. While this dependency complicates the quantification of tissue concentrations in myocardium it actually can be utilized for the measurement of systolic wall thickening. As shown recently in our laboratory the counts recovered from a given myocardial segment and expressed in counts/min/gram tissue increase from enddiastole to endsystole. This increase was found to be proportional to the degree of wall thickening as determined by echocardiography. If applied to man, regional myocardial blood flow measurements therefore could be combined with determinations of regional mechanical function and both measurements easily correlated. It would also seem feasible to expand this concept to the correlation of regional myocardial function with metabolism provided the myocardium is visualized with a metabolic tracer.

c) Assessment of regional metabolism

FREE FATTY ACID METABOLISM: Free fatty acids are the main energy substrates of the heart and preferentially extracted by myocardium. It therefore seemed only logical to employ radioactive labeled fatty acids or fatty acid analogs for external myocardial imaging. Evans and coworkers⁽²⁴⁾ were the first to radioiodinate oleic acid and to demonstrate its utility for gamma camera imaging of the heart. More recently, palmitic acid has been labeled with carbon-11, a procedure that does not alter the biological behavior of this fatty acid and has been used extensively for tomographic imaging of the heart by PCT^(25,26). With this imaging agent the group at Washington University in St. Louis has succeeded in quantification of acute myocardial infarction in the experimental animal⁽²⁷⁾ as well as in man⁽²⁸⁾.

Beyond its sole use for myocardial imaging this agent may eventually allow quantification of regional myocardial fatty acid metabolism. The uptake of this agent in myocardium or its turnover rates should be related to the rate of fatty acid utilization. Studies by Goldstein et al⁽²⁹⁾ and Klein et al⁽³⁰⁾ seem in fact to confirm this hypothesis. Using the isolated perfused rat heart, these investigators observed a close relationship between cardiac work and myocardial half times of C-11 palmitic acid. For example, at high work loads, the myocardial half times of C-11 palmitate were significantly shorter than at low work loads suggesting greater utilization of fatty acids in myocardium when energy demand is high. While these observations are indeed intriguing their application in the in vivo situation with indicator recirculation and flow dependency of indicator delivery and washout appears complex and awaits further validation.

In addition to C-11 labeled fatty acids, a number of fatty acid analogs have been synthesized. Instead of the relatively short lived C-11 these analogs employ Fluorine-18 with a half time of nearly two hours. Use of

Flourine-18 labeled compounds, e.g. F-18 hexadecanoic acid or F-18 heptadecanoic acid^(31,32), may to some degree obviate the necessity for on-site production. The nearly 2 hour half time permits production in a centrally located cyclotron and subsequent delivery to users in nearby medical centers. While initial results with these analogs are promising, e.g. their kinetics in myocardium resemble to some degree that of the physiologic palmitic acid, their ultimate utility for the assessment of myocardial fatty acid metabolism has not been demonstrated yet.

GLUCOSE METABOLISM: We have discussed earlier several of the radionuclides that can be labeled to naturally occurring compounds without affecting their biologic behavior. Accordingly, one could label for example glucose, which together with free fatty acids is a primary energy substrate of the heart. While this can easily be accomplished, the chemical state of this radioactive agent however at any time after intravenous administration remains unknown to the PCT. The measured C-11 tissue concentrations would represent a complex distribution of compounds that further changes with time. Moreover, the rapid turnover rate of glucose in myocardium poses some limitations for obtaining high contrast cross-sectional images.

It is conceivable that ultimately the complex kinetics of some natural compounds cannot be defined sufficiently for accurate measurements of myocardial metabolic rate and that we must resort to substrate analogs that trace only one segment of a metabolic pathway but that can be delineated well and their kinetics expressed in form of a physiologic model and described in mathematical terms. An example of this is the radioactive labeled 2-deoxyglucose which has become available as a substrate analog for the measurement of regional glucose utilization rates. Sokoloff and associates⁽³³⁾ labeled this agent with C-14 and originated a physiologic model that permitted the

measurement of local cerebral glucose utilization in vitro. This technique was adopted for in vivo PCT measurements after the 2-hydroxy group was substituted by an F-18 atom to yield F-18 2-fluoro-2-deoxyglucose (FDG) (34,35). Further, the original physiologic model was modified in our laboratory by Huang et al (36) and measurements of regional cerebral glucose metabolism by this approach validated by Phelps et al (37). Once administered intravenously, exchange of FDG across the capillary and cell membranes as well as initial metabolization is similar and in proportion to glucose. Like glucose, it is phosphorylated by hexokinase to FDG-6-PO_4 but becomes metabolically trapped and is not a substrate for glycolysis, glycogen formation or the pentose shunt. Metabolically unbound FDG subsequently clears from myocardium and PCT images obtained at equilibrium reflect the regional utilization rates of exogenous glucose.

The kinetics of FDG can be expressed by a three-compartmental tracer kinetic model with exchange between compartments that follows first order of kinetics. This is shown schematically in figure 8, where k_1^* and k_2^* are the rate constants for forward and reverse transport across the capillary membrane and k_3^* and k_4^* the rate constants for phosphorylation and dephosphorylation between FDG and FDG-6-PO_4 . Our initial findings suggest that these rate constants are in myocardium of similar magnitude as those in the brain (38). Once established they will be incorporated together with the physiologic model into the tomograph's systems program so that regional myocardial glucose utilization rates can be determined routinely and almost entirely by trained nuclear medicine technicians. For this measurement, FDG is administered intravenously and venous blood sampled serially. After forty to fifty minutes, at near steady state conditions, cross-sectional imaging is performed, plasma glucose and FDG levels obtained and entered into the tomograph's systems computer with automatic calculation of regional myocardial

glucose utilization rates from selected regions of interest. The accuracy of these measurements has been documented for the brain but awaits validation for the heart. Nevertheless, our initial experience has been encouraging⁽³⁹⁾. Regional glucose utilization rates calculated by this noninvasive approach ranged from 4 to 16 mg glucose/min/100gm and were in close agreement with measurements derived invasively in our laboratory in animal experiments using the Fick-method (Phelps, unpublished data).

C. POTENTIAL CLINICAL APPLICATIONS

Thus far, we have discussed only the technical aspects of "physiologic tomography", i.e. the tomographic imaging for the noninvasive quantification of local myocardial blood flow, mechanical function and metabolism^(40,41). Considering the complexities, effort and cost involved, the question as to whether this new study means will become clinically feasible and cost effective seems appropriate. Our initial experience with this new tool in patients with cerebral disease is very encouraging and suggests that metabolic abnormalities of the brain detected by physiologic tomography provide indeed an improved understanding of cerebral function⁽⁴²⁾. Moreover, local metabolic alterations did explain or substantiate the clinical symptomatology to a far better than the structural abnormalities determined by CT scanning. To what degree this will apply to the heart is at present uncertain and will have to be answered in the near future.

Nevertheless, "physiologic tomography" offers a unique and heretofore unknown potential for the study of regional myocardial physiology and pathophysiology. Regarding its future role in the clinical situation, we have demonstrated in the experimental animal, that it is possible to detect coronary stenoses of less than 50% diameter narrowing with PCT and N-13 ammonia during pharmacologically induced coronary vasodilatation⁽⁴³⁾. We are cur-

rently extending these observations to man.

It is known that even moderately severe coronary stenoses may not affect resting coronary blood flow yet limit coronary flow reserve. More importantly, coronary flow reserve can be reduced by even very mild stenoses, a phenomenon which can be demonstrated during maximum coronary vasodilatation (44). This principle was employed in the chronically instrumented animal - as mentioned above - and is now used in our institution in man. Our results to date in 12 normal volunteers and 29 patients with arteriographically documented coronary artery disease appear to confirm the animal experimental findings and indicate that coronary stenoses as low as 40% diameter narrowing can be identified. Among the patients there were 11 with single vessel disease, 8 with double vessel disease and 10 with triple vessel disease. All 12 normal volunteers had normal studies at rest and during pharmacologically induced hyperemia. By contrast, among the 29 patients with arteriographically documented coronary artery disease, hyperemia induced new or more extensive perfusion abnormalities in 28. Of the 11 patients with single vessel disease 10 were accurately diagnosed by this technique and the one patient with a false positive study had a stenosis of the right coronary artery with adequate perfusion of the inferior wall from the left circumflex coronary artery. Taken together, all 29 patients had a total of 57 stenosed vessels and of those, 49 were accurately identified by PCT and N-13 ammonia during pharmacologically induced hyperemia (Figure 9) (45).

Stenoses that were not detected were usually the least severe ones. In this particular study, image analysis was qualitative rather than quantitative. In other words, the myocardial segment with the highest increase in activity during hyperemia served as a reference. In the future, however, it might be possible to determine the change in regional myocardial blood flow

from control to hyperemia more quantitatively (22). If for example in normals dipyridamole produces a consistent and reproducible increase in coronary blood flow then the failure to or an only partial increase in a given myocardial segment should indeed indicate the presence of a coronary stenosis and could be detected by a more quantitative assessment of regional myocardial blood flow or its changes by PCT and N-13 ammonia. This then would permit a quantitative assessment of the coronary flow reserve for any given myocardial segment.

As another example, this new study technique may permit for the first time characterization of the local metabolic alterations associated with acute myocardial ischemia. In a preliminary series of animal experiments (46) we applied a graded stenosis to the left anterior descending coronary artery and induced ischemia by pacing at high rates. Myocardial perfusion assessed with N-13 ammonia and PCT was reduced in the ischemic segment. FDG concentrations as an index of regional glucose utilization similarly were decreased in the ischemic segment, yet disproportionately less than the reduction in flow (Figure 10). Quantitative correlation between perfusion and the glucose uptake on the cross-sectional images demonstrated in the ischemic segments that glucose uptake occurred in excess of flow. If blood flow closely reflects the oxygen availability (i.e. if oxygen extraction does not significantly increase at low flows) then these observations suggest that in the ischemic segment energy is primarily derived from glucose either by residual oxidative capacity and/or anaerobic glycolysis. This would be in agreement with earlier findings obtained in acute and destructive animal experiments (47). Should this approach be applicable to man it then may become possible to identify ischemic myocardium, characterize its metabolic state, perhaps its degree of viability, and to assess the benefits of

interventions designed to salvage injured myocardium. Since the severity of ischemia not only depends upon blood flow but also on the mechanical demand as well as on the duration of the insult - all of which are at present difficult if not impossible to assess - "physiologic tomography" may indeed provide the most accurate means for estimating the degree of ischemia.

SUMMARY

The examples described above were intended to illustrate the potential of "physiologic tomography" and to describe the type of information that can be obtained. It is conceivable that such data may prove to be clinically useful and relevant. Nevertheless, and as mentioned earlier, the utility and ultimate role of this new imaging modality in health care delivery is difficult to assess at present and needs to be defined in the future. It would seem to us however that with the improvements in instrumentation and the development of a compact, reliable and generator-like cyclotron physiologic tomography will become more readily accessible to a larger number of users. There can be little doubt that physiologic tomography represents an important new tool for investigative studies to improve our understanding of cardiac physiology and disease. The quantitative aspects as well as simultaneous evaluation of more than one segment of myocardial performance, e.g. simultaneous study of mechanical function, blood flow and metabolism and their interdependency will provide new insights into myocardial physiology. Because many of the cardiovascular disorders may originate at the cellular or metabolic level it is hoped that this technique may serve as a means for the early detection of cardiac disease, perhaps at a stage when it is still amenable to therapy.

REFERENCES

1. Phelps, M.E.: Emission computed tomography. Sem. Nucl. Med. 7:337-365, 1977.
2. Weiss, E.S., Siegel, B.A., Sobel, B.E., Welch, M.J. and Ter-Pogossian, M.M.: Evaluation of myocardial metabolism and perfusion with positron-emitting radionuclides. In: Principles of Cardiovascular Nuclear Medicine (ed. by Holman, B.L., Sonnenblick, E.H. and Lesch, M.), Grune and Stratton, New York, 1979, pp. 66-82.
3. Budinger, T.F. and Rollo, F.D.: Physics and instrumentation. In: Principles of Cardiovascular Nuclear Medicine (ed. by Holman, B.L., Sonnenblick, E.H. and Lesch, M.) Grune and Stratton, New York, 1979, pp. 17-52.
4. Phelps, M.E., Hoffman, E.J., Huang, S.C. and Kuhl, D.E.: ECAT: A new computerized tomographic imaging system for positron emitting radiopharmaceuticals. J. Nucl. Med. 19:635-647, 1978.
5. Hoffman, E.J., Phelps, M.E., Wisenberg, G., Schelbert, H.R. and Kuhl, D.E.: ECG gating in positron emission computed tomography. J. Comp. Tomogr. (in press).
6. Grant, P.M., Erdal, B.R., O'Brien, H.A.: A ^{82}Sr - ^{82}Rb isotope generator for use in nuclear medicine. J. Nucl. Med. 16:300-304, 1975.
7. Hnatowich, D.J.: A method for the preparation and quality control of ^{68}Ga radiopharmaceuticals. J. Nucl. Med. 16:764-768, 1975.
8. Ku, T.H., Richards, P., Stang, L.G. and Prach, T.: Generator production of manganese-52m for positron tomography. J. Nucl. Med. 20:682, 1979 (abstract).

9. Robinson, J.D.: Copper 62: a short-lived, generator produced, positron emitting radionuclide for radiopharmaceuticals. J. Nucl. Med. 17:559, 1976 (abstract).
10. Gelbard, A.S., Clarke, L.P., McDonald, M.J.: Enzymatic synthesis and organ distribution studies with ^{13}N -labeled L-glutamine and L-glutamic acid. Radiology 116:127-132, 1975.
11. Hoffman, E.J. and Phelps, M.E.: Quantitation in positron emission tomography I. Effect of object size. J. Comp. Tomogr. 3:299-308, 1979.
12. Wisenberg, G., Schelbert, H., Selin, C., Hoffman, E., Huang, H. and Phelps, M.: The use of positron emission tomography to quantify regional myocardial blood flow. Circulation 59/60, Suppl II:268, 1979 (abstract).
13. Hnatowich, D.J.: Labeling of tin-soaked albumin microspheres with ^{68}Ga . J. Nucl. Med. 17:57-60, 1976.
14. Heymann, M.A., Payne, B.D., Hoffman, E.J. and Rudolph, A.M.: Blood flow measurements with radionuclide-labeled particles. In: Principles of Cardiovascular Nuclear Medicine (ed. by Holman, B.L., Sonnenblick, E.H. and Lesch, M.) Grune and Stratton, New York 1979, p. 135-139.
15. Myers W.G.: Radiopotassium-38 for in vivo studies of dynamic processes. J. Nucl. Med. 14:359-360, 1973.
16. Budinger, T.F., Yano, Y., Derenzo, S.E., Huesman, R.H. Cahoon, J.L., Moyer, B.R., Greenberg, W.L. and O'Brien, H.A.: Rb-82 myocardial positron emission tomography. J. Nucl. Med. 20:603, 1979 (abstract).
17. Mack, S.N., Eichling, J.O., Bergmann, S.R. and Sobel, B.E.: External quantification of perfusion. Circulation 59/60, Suppl II:269, 1979 (abstract).
18. Hunter, W. and Monahan, W.G.: ^{13}N -ammonia: A new physiologic radiotracer for nuclear medicine (abstract) J. Nucl. Med. 12:368, 1971.

19. Harper, P.V., Lathrop, K.A., Krizek, H., Lembares, N., Stark, V. and Hoffer, P.B.: Clinical feasibility of myocardial imaging with $^{13}\text{NH}_3$. J. Nucl. Med. 13:278-280, 1972.
20. Phelps, M.E., Hoffman, E.J., Coleman, R.E., Welch, M.J., Raichle, M.E., Weiss, E.S., Sobel, B.E. and Ter-Pogossian, M.M.: Tomographic images of blood pool and perfusion in brain and heart. J. Nucl. Med. 17:603-612, 1976.
21. Phelps, M.E., Hoffman, E.J. and Raybaud, C.: Factors which affect cerebral uptake and retention of $^{13}\text{NH}_3$. Stroke 8:694-702, 1977.
22. Schelbert, H.R., Phelps, M.E., Hoffman, E.J., Huang, S.C., Selin, C.E. and Kuhl, D.E.: Regional myocardial perfusion assessed with N-13 labeled ammonia and positron emission computerized axial tomography. Am. J. Cardiol. 43:209-218, 1979.
23. Schelbert, H.R., Phelps, M., Robinson, G., Huang, S., Hoffman, E. and Selin, C.: N-13 ammonia for the non-invasive measurement of myocardial blood flow. J. Nucl. Med. 20:603, 1979 (abstract).
24. Evans, J.R., Gunton, R.W., Baker, R.G., Beanlands, D.S. and Spears, J.C.: Use of radioiodinated fatty acid for photo-scans of the heart. Circ. Res. 16:1-10, 1965.
25. Hoffman, E.J., Phelps, M.E., Weiss, E.S., Welde, M.J., Coleman, R.E., Sobel, B.E., Ter-Pogossian, M.M.: Transaxial tomographic imaging of canine myocardium with ^{11}C -palmitic acid. J. Nucl. Med. 18:57-61, 1977.
26. Weiss, E.W., Hoffman, E.J., Phelps, M.E., Welch, M.J., Henry, P.D., Ter-Pogossian, M.M. and Sobel, B.E.: External detection and visualization of myocardial ischemia with ^{11}C -palmitic acid. Circ. Res. 39:24-32, 1976.

27. Weiss, E.S., Ahmed, S.A., Welch, M.J., Williamson, J.R., Ter-Pogossian, M.M. and Sobel, B.E.: Quantification of infarction in cross sections of canine myocardium in vivo with positron emission transaxial tomography and ^{11}C -palmitate. *Circulation* 55:66-73, 1977.
28. Klein, M.S., Ter-Pogossian, M.M., Markham, J., Roberts, R., Sobel, B.E.: Quantification of infarction by positron emission tomography in man. *Circulation* 59/60, Suppl II:268, 1979 (abstract).
29. Goldstein, R.A., Klein, M.E. and Sobel, B.E.: External quantification of myocardial metabolism in vivo. *Circulation* 57/58, Suppl II:4, 1978 (abstract).
30. Klein, M.W., Goldstein, R.A., Tewson, T.J., Welch, M.J. and Sobel, B.E.: Noninvasive quantitation of myocardial metabolism with intravenous and intraatrial injections of ^{11}C palmitate. *Am. J. Cardiol.* 43:356, 1979 (abstract).
31. Machulla, H.J., Stocklin, G., Kupfernagel, Ch., Hock, A., Vyska, K.: Comparative evaluation of fatty acids labeled with C-11, Cl-34m, Br-77, and I-123 for metabolic studies of myocardium. Concise communication. *J. Nucl. Med* 19:298-302, 1978.
32. Knust, E.J., Kupfernagel, Ch. and Stocklin G.: Long-chain F-18 fatty acids for the study of regional metabolism in heart and liver; odd-even effects of metabolism in mice. *J. Nucl. Med.* 20:1170-1175, 1979.
33. Sokoloff, L., Reivich, M., Kennedy, C., Des Rosiers, M.H., Patkla, C.S., Pettigrew, K.D., Sakurada, O., and Shinohara, M.: The (^{14}C) deoxyglucose method for the measurement of local cerebral glucose utilization. Theory, procedure and normal values in conscious and anesthetized rats. *J. Neurochem.* 28:897-916.

34. Gallagher, B.M., Ansari, A., Atkins, H., Casella, V., Christman, D.E., Fowler, J.S., Ido, T., MacGregor, R.R., Sam, P., Wan, C.N., Wolf, A.P., Kuhl, D.E. and Reivich, M.: Radiopharmaceuticals XXVII. ^{18}F labeled 2-deoxy-2-fluoro-D-glucose as a radiopharmaceutical for measuring regional myocardial glucose metabolism in vivo. Tissue distribution and imaging studies in animals. *J. Nucl. Med.* 18:990-996, 1977.
35. Reivich, M., Kuhl, D.E., Wolf, A., Greenberg, J., Phelps, M., Ido, T., Casella, V., Fowler, J., Hoffman, E., Alavi, A. Som, P. and Sokoloff, L.: Measurement of local cerebral glucose utilization in man with ^{18}F -2-fluoro-2-deoxy-D-glucose. *Circ. Res.* 44:127-137, 1979.
36. Huang, S.C., Phelps, M.E., Hoffman, E.J., Sideris, K., Selin, C.E. and Kuhl, D.E.: Non-invasive determination of local cerebral metabolic rate of glucose in man with (F-18)-fluoro-2-deoxyglucose and emission computed tomography: Theory and results. *Am. J. Physiol.* (in press).
37. Phelps, M.E., Huang, S.C., Hoffman, E.J., Selin, C., Sokoloff, L. and Kuhl, D.E.: Tomographic measurement of local cerebral glucose metabolic rate in man with 2-(^{18}F)fluoro-2-deoxy-D-glucose: Validation of the method. *Ann. Neurol.* 6:371-388, 1979.
38. Phelps, M.E., Hoffman, E.J., Selin, C., Huang, S.C., Robinson, G., MacDonald, N., Schelbert, H.R. and Kuhl, D.E.: Investigation of ^{18}F -2-Fluoro-2-Deoxyglucose for the Measure of Myocardial Glucose Metabolism. *J. Nucl. Med.* 19:1311-1319, 1978.
39. Phelps, M.E., Schelbert, H.R., Hoffman, E.J., Huang, S.C. and Kuhl, D.E.: Physiologic tomography of myocardial glucose metabolism, perfusion and blood pools with multiple gated acquisition. *Clin. Cardiol.* (in press).

40. Phelps, M.E., Hoffman, E.J., Huang, S.C. and Kuhl, D.E.: Positron Tomography: An In vivo autoradiographic approach to the measurement of cerebral hemodynamics and metabolism. In: Cerebral Function, Metabolism and Circulation. (ed. by Ingvar, D.H., Lassen, N.A.) 446-447, 1977. (Acta Neuro. Scand. 56, Munksgaard, Copenhagen, pp. 178-179,
41. Phelps, M.E., Hoffman, E.J. and Huang, S.C.: Physiologic tomography: A new approach to in vivo measure of metabolism and physiologic function. In: Medical Radionuclide Imaging, Vol. 1, Vienna, IAEA, 233-253, 1977.
42. Kuhl, D.E., Phelps, M.E., Kowell, A.P., Metter, E.J., Selin, C. and Winter, J.: Mapping Local Metabolism and Perfusion in Normal and Ischemic Brain by Emission Computed Tomography of ^{18}F FDG and ^{13}N NH_3 . Annal. Neurol. (in press).
43. Gould, K.L., Schelbert, H.R., Phelps, M.E. and Hoffman, E.J.: Non-invasive assessment of coronary stenosis by myocardial perfusion imaging during pharmacologic coronary vasodilatation. V. Detection of 47% diameter coronary stenosis with intravenous N-13 ammonia and emission computed tomography in intact dogs. Am. J. Cardiol. 43:200-208, 1979.
44. Gould, K.L., Lipscomb, K. and Hamilton, G.W.: Physiologic basis for assessing critical coronary stenosis. Instantaneous flow response and regional distribution during coronary hyperemia as measures of coronary flow reserve. Am. J. Cardiol. 33:87-94, 1974.
45. Schelbert, H., Wisenberg, G., Gould, L., Marshall, R., Phelps, M.E., Hoffman, E., Gomes, A. and Kuhl, D.: Detection of Coronary Artery Stenosis in Man by Positron Emission Computed Tomography and N-13 Ammonia. Circ. 59/60, Suppl II:60, 1979.

46. Schelbert, H.R., Phelps, M.E., Selin, C., et al: Regional myocardial ischemia assessed by ^{18}F -fluoro-2-deoxyglucose and positron emission computed tomography. Clin. Cardiol. (in press).
47. Opie, L.H., Owen, P. and Riemersma, R.A.: Relative rates of oxidation of glucose and free fatty acids by ischemic and non-ischemic myocardium after coronary artery ligation in the dog. Eur. J. Clin. Invest. 3:419-435, 1973.

LEGENDS

Figure 1: Annihilation coincidence detection. The figure schematically shows a cross section through the chest and a pair of scintillation detectors (D) connected by an electronic coincidence circuitry. Interaction 1 between a positron and an electron results in two 511 KeV photons that are emitted in diametrically opposed directions and detected by the pair of detectors. The total attenuation A for the two photons is a function of the sum of their path lengths a and b and the tissue specific attenuation coefficient μ . Only interactions that occur in the field between the two detectors are recorded and this accounts for the depth-independent resolution. Interactions 2 and 3 remain undetected by the detector pair.

Figure 2: Prototype transaxial positron emission tomographs. A: two single crystal detector heads; and B: two banks with multiple detectors rotating around patient. C: Hexagonal; and D: circular array of scintillation detectors.

Figure 3: Commercial version of a positron emission transaxial computed tomograph (hexagonal array) in the Nuclear Medicine Clinic at the University of California, Los Angeles (see text). (With permission of the Journal of Nuclear Medicine).

Figure 4: Sequence of cross-sectional images of the left ventricular myocardium obtained after injection of N-13 ammonia in a normal volunteer. The cross sections are spaced apart 1cm. Cross sections 1 and 2 show the high anterior wall of the left ventricle, cross sections 3 - 5 transverse the mid left ventricle and cross section 6 is a diagonal cut through the diaphragmatic portion of the left ventricle.

Figure 5. Gated enddiastolic (A) and endsystolic (B) cross-sectional images of the left ventricular myocardium obtained after administration of F-18

deoxyglucose in a healthy volunteer (ANT and POST = anterior and posterior; L and R = right and left).

Figure 6. Changes in regional myocardial N-13 ammonia concentrations in response to changes in regional myocardial blood flow. This sequence of images was obtained at the same level through the left ventricular myocardium in the same dog at one hour intervals to allow for sufficient decay of short-lived N-13 to near undetectable levels and after repeat injections of N-13 ammonia for each image. Cross section 1 was recorded after N-13 ammonia was injected at control; cross sections 2 and 3 while flow in the left anterior coronary artery was increased by intracoronary papaverine to 50% and 610% above control. The increase in activity noted in the anterior wall (arrows) is associated with the increase in left-anterior descending coronary artery flow. Cross section 4 was obtained after a fourth injection of N-13 ammonia during acute reduction of flow in the left anterior descending coronary artery.

Figure 7: Relationship between myocardial N-13 ammonia tissue concentrations and myocardial blood flow (MBF) in dogs determined by in vitro tissue counting. Note the nearly linear response within the range of physiologically occurring flows (with permission of the American Journal of Cardiology).

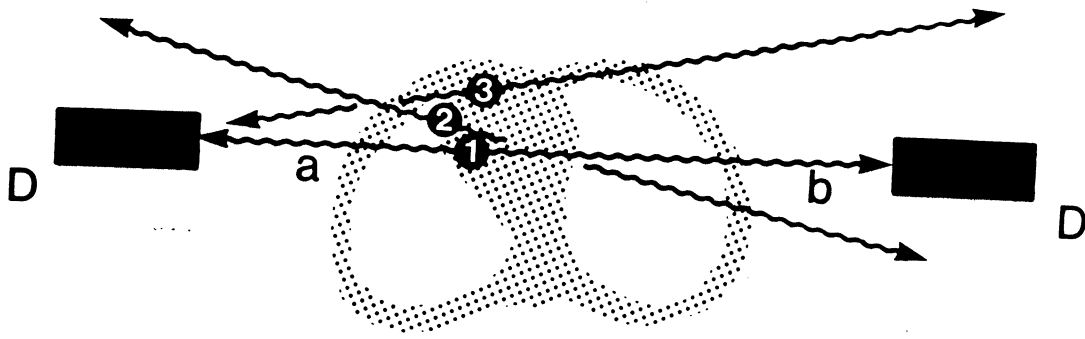
Figure 8: Three compartmental model for the exchange of F-18 deoxyglucose (see text).

Figure 9: Cross-sectional images of the distribution of myocardial blood flow in left ventricular myocardium at control (A) and during dipyridamole induced coronary hyperemia (B) in a patient with left anterior descending coronary artery stenosis. (ANT and POST = anterior and posterior; L and R = left and right). Cross section 1 shows the high anterior wall, cross section 2 the mid and cross section 3 the diaphragmatic portion of the left ventricle. Note the

uniform distribution of activity at control which becomes abnormal during hyperemia because flow in the distribution of the left anterior descending coronary artery failed to increase adequately (arrows).

Figure 10: Three cross-sectional images of the regional left ventricular myocardial blood flow (Panel B; visualized by N-13 ammonia) and glucose utilization (Panel B; visualized by F-18 deoxyglucose) during pacing induced ischemia in a dog (see text). Note the partial mismatch in the anterior wall between the flow and glucose image as indicated by the arrows.

Acknowledgement: The authors deeply appreciate Maureen A. Kinneys secretarial skills in preparing this manuscript.



$$A = e^{-\mu(a+b)}$$

Figure 1.

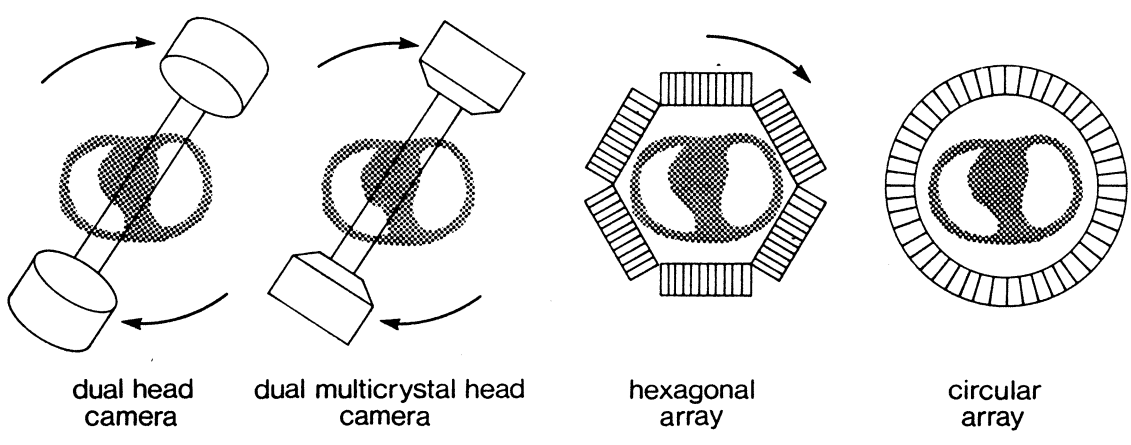


Figure 2.

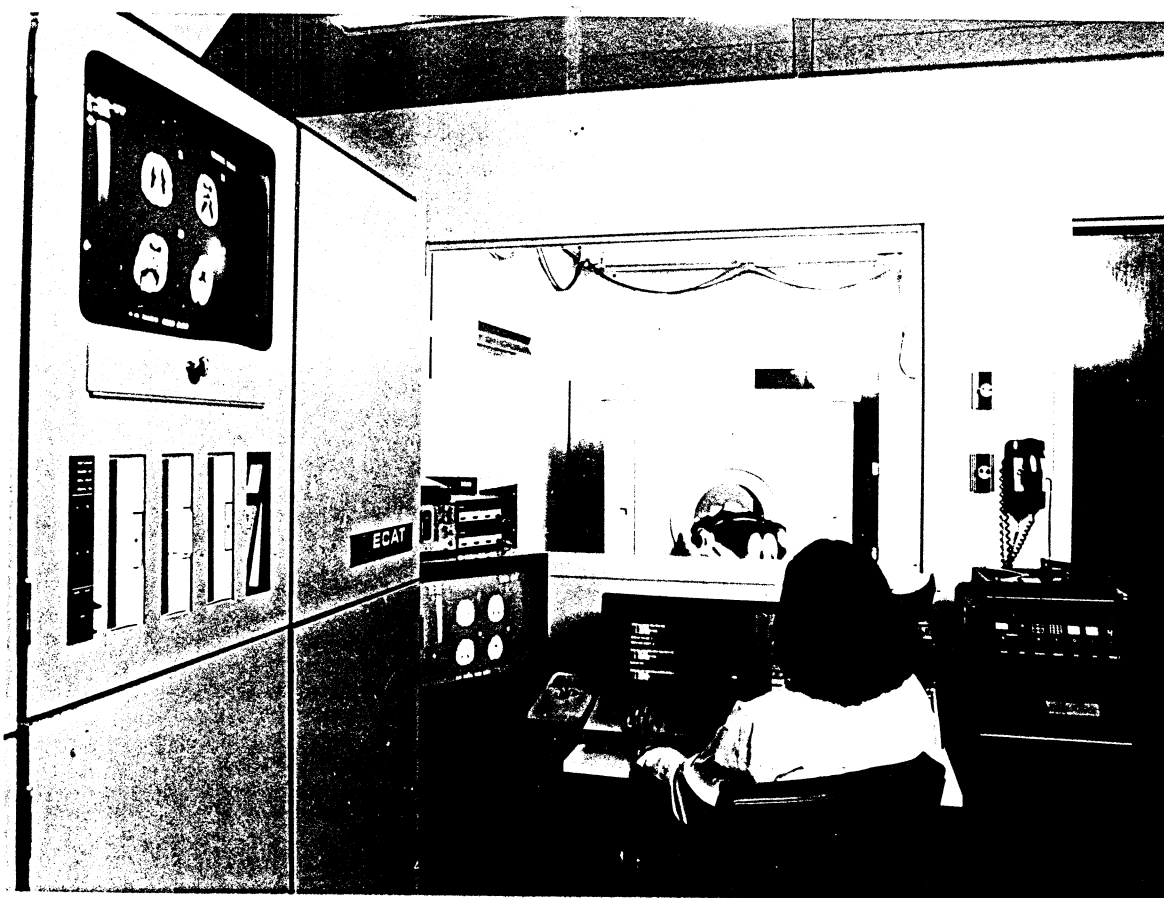


Figure 3.

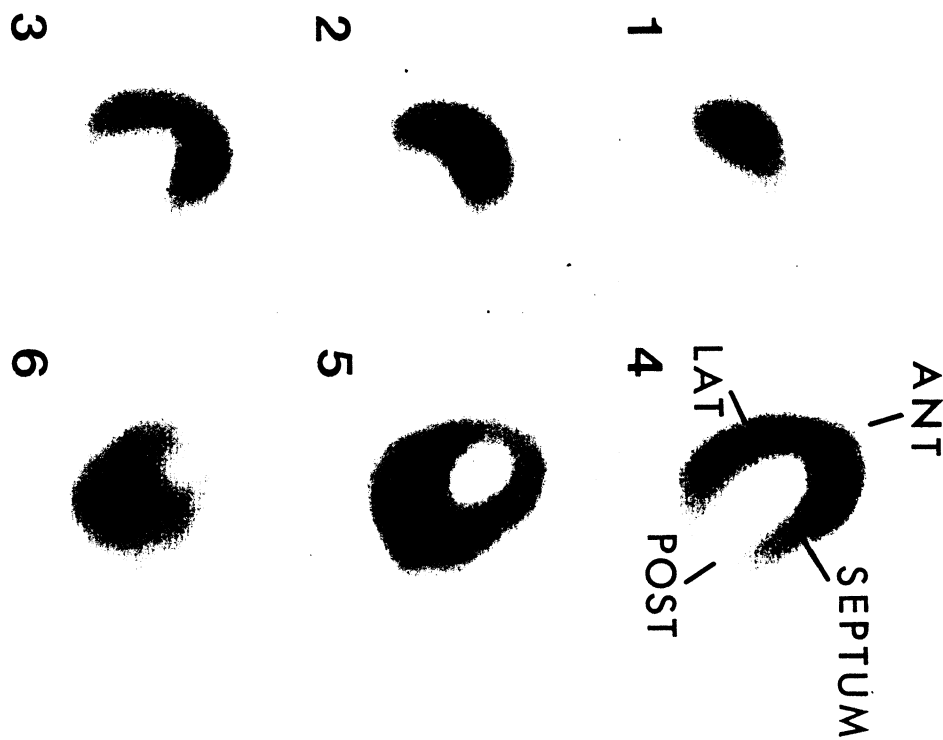


Figure 4.

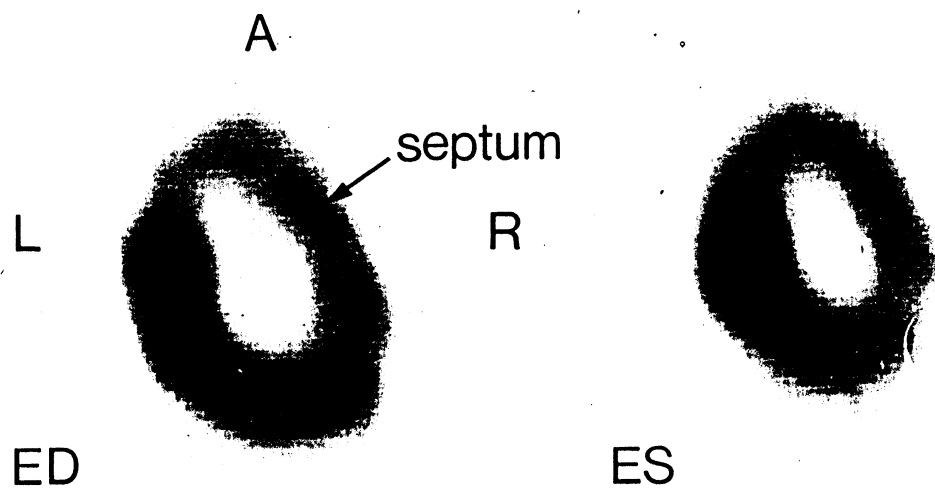


Figure 5.

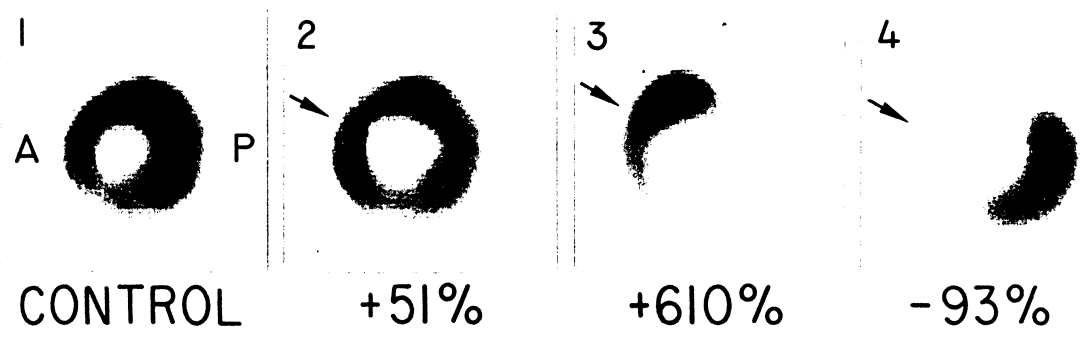


Figure 6.

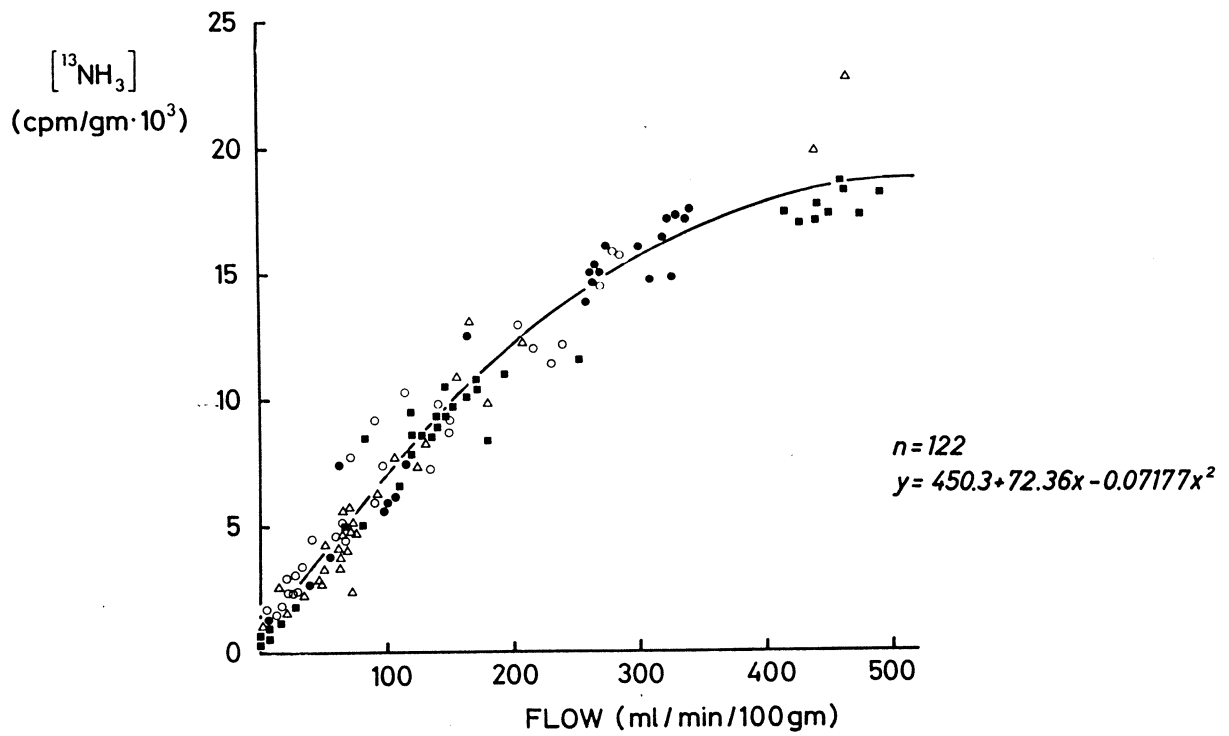


Figure 7.

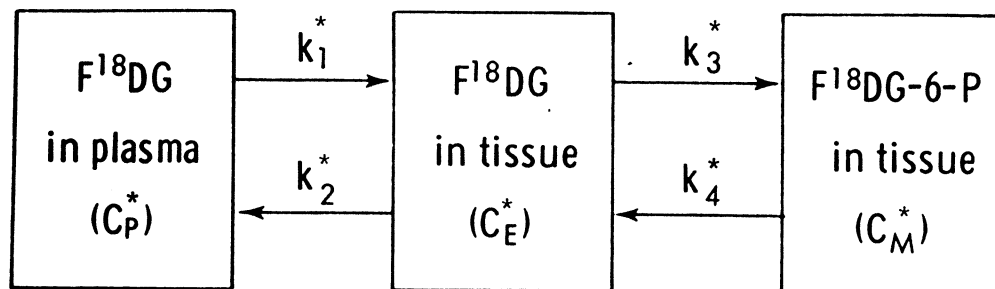


DIAGRAM OF THE THREE COMPARTMENTS IN FDG MODEL

Figure 8.

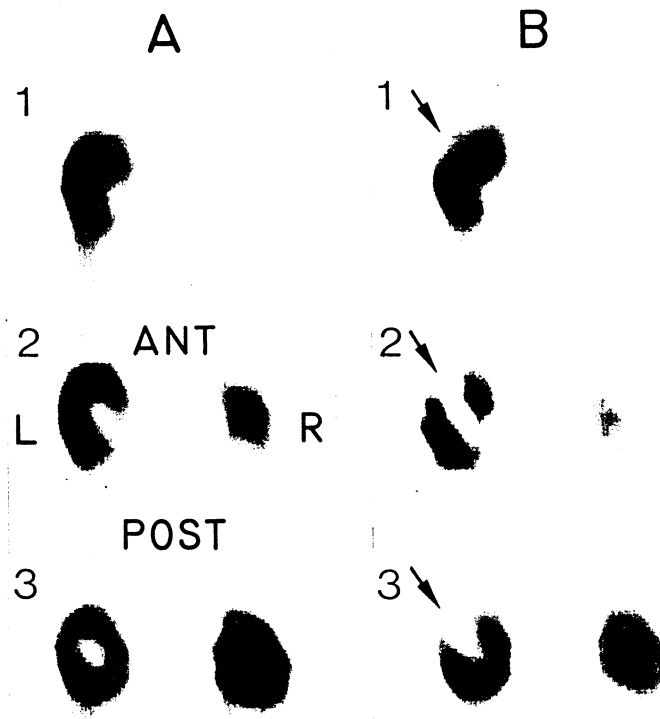


Figure 9.

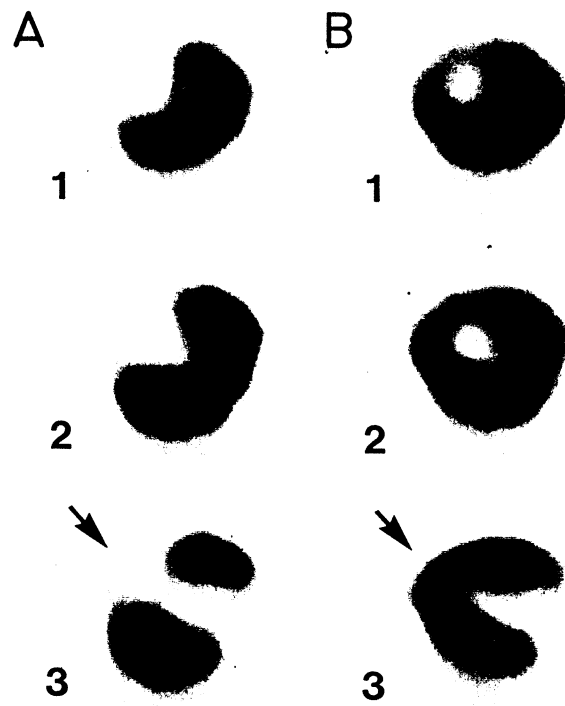


Figure 10.